BIODEGRADABLE NANOPARTICLES LOADED WITH TETRAMERIC MELITTIN: PREPARATION AND MEMBRANE DISRUPTION EVALUATION

Azucena Gonzalez-Horta[1♱*], Arely Matamoros-Acosta[1♱], Abelardo Chavez-Montes[2], Rocio Castro-Rios[3], Jorge Lara-Arias[4]

[1]Laboratory of Genomic Science, Faculty of Biological Sciences, Universidad Autonoma de Nuevo Leon, 66451 San Nicolas de los Garza, N.L. Mexico

[2]Department of Chemistry, Faculty of Biological Sciences, Universidad Autonoma de Nuevo Leon, 66451 San Nicolas de los Garza, N.L. Mexico

[3]Department of Analytical Chemistry, Faculty of Medicine, Universidad Autonoma de Nuevo Leon, 66451 San Nicolas de los Garza, N.L. Mexico

[4]Bone and Tissue Bank, University Hospital Dr. Jose E. Gonzalez, Monterrey, Mexico

♱ These authors have contributed equally to this paper

*Corresponding author: Azucena Gonzalez-Horta

Laboratory of Genomic Science

Faculty of Biological Science

Universidad Autonoma de Nuevo Leon

66451 Monterrey, N.L. MEXICO

Email: azucena.gonzalezhr@uanl.edu.mx

Phone: +52 8183294110

SUMMARY

Melittin is the main component of bee venom consisting of 26 amino acid that has multiple effects, including antibacterial, antiviral and anti-inflammatory in various cell types. This peptide forms pores in biological membranes and triggers cell death. Therefore it has potential as an anti-cancer therapy. However the therapeutic application of melittin is limited due to its main side effect, hemolysis, which is especially pronounced following intravenous administration. In the present study, we formulated tetrameric melittin-carrying poly-D,L-lactic-co-glycolic acid nanoparticles (PLGA-NPs) and analyzed the lytic activity of this system on liposomes that resembles breast cancer cells. Tetrameric melittin binds avidly to PLGA nanoparticles with an encapsulation efficiency of 97% and retains its lytic activity demonstrating the effectiveness of PLGA nanoparticles as nanocarriers for this cytolytic peptide.

Keywords: melittin, PLGA nanoparticles, liposomes, leakage, fluorescence, circular dichroism.

Introduction

Melittin is a naturally occurring cationic antimicrobial peptide obtained from the toxic component in the venom of the European honey bee, *Apis mellifera* (1). It is a small linear peptide composed of 26 amino acids having the sequence NH_2-GIGAVLKVLTTGLPALISWIKRKRQQ-$CONH_2$. The amino-terminal region (residues 1-20) of this peptide is predominantly hydrophobic whereas the carboxy-terminal region (residues 21-26) is hydrophilic due to the presence of a stretch of positively charged amino acids (2). Due to this amphiphilic property of melittin it becomes water-soluble and spontaneously associates with natural and artificial membranes (3). Because of poor cell selectivity, it exhibits strong lytic activity against both bacterial and mammalian cells (4). Melittin is intrinsically fluorescent due to the presence of a single tryptophan residue at the 19th position. The presence of this tryptophan is utilized as the probe to study the interaction of the peptide with membranes and membrane-mimetic systems (5). Melittin's action was thought to involve membrane pore formation or membrane perturbation, resulting in the disruption of the membrane (6-8). This peptide is an attractive anticancer candidate because of its wide-spectrum lytic properties. Although cytotoxic to a broad spectrum of tumor cells (9-11) melittin is also toxic to red blood cells and its therapeutic potential cannot be achieved without a proper delivery vehicle. This could be overcome by melittin nanoparticles that possess the ability to safely deliver a significant amount of melittin and to target and kill cancer cells. In recent years, nanoparticles (NPs) were prepared from biodegradable polymers such as poly-D,L-lactic-co-glycolic acid (PLGA), a copolymer of lactic and glycolic acid approved by FDA for certain clinical uses. The polymer degradation time can vary from several months to years, depending on the molecular weight and

copolymer ratio. PLGA is nontoxic, nonirritating and fully biodegradable with good biocompatibility and human adaptability. *In vivo*, the final degradation product of PLGA is lactate that can be metabolized by intravital cells (12). Also, the physicochemical properties of bee venom-loaded PLGA NPs has been characterized in order to design and optimize a suitable sustained release system (13) however the melittin lytic activity on unilamellar lipid bilayer (liposomes) once incorporated into NP has not been evaluated. Liposomes are synthetic mimics of cellular membranes and represent an experimental system widely used for more than 30 years in the field of biochemical research involving lipids. Another promising solution to reduce melittin´s cytotoxicity is to introduce cell selectivity by modulating melittin assembly and its inherent secondary structure in the aqueous environment of the bloodstream (14). In this study, we have performed spectroscopic studies aimed at disclosing the basic structural characteristics of tetrameric melittin after been incorporated into PLGA-NP.

Materials and Methods

Materials

Melittin was from Sigma Aldrich chemicals (Saint, Louis, MO) stock solution was dissolved in 10mM Hepes (Sigma Aldrich chemicals, Saint Louis, MO) buffer, NaCl 150mM pH 7.4 at final concentration of 1.7mM. The resulting melittin solution (5mg/mL) was then frozen and kept at -20ºC until used. The lipids L-α-phosphatidylcholine from egg yolk (PC), 1,2-Diacyl-*sn*-glycero-3-phosphatidylethanolamine (PE), L-α-Phosphatidic acid sodium salt (PA) and 1,2-Diacyl-*sn*-glycero-3-phospho-L-serine (PS) were from Avanti polar lipids (Alabaster, AL). PLGA (MW

50,000-75,000: lactide-co-glycolide ratio 85:15) was from Sigma Aldrich (Saint Louis, MO). ANTS (8-aminonaphthalene-1,3,6-trisulphonic acid) and DPX (N,N'-p-xylene-bis-pyrimidinium bromide) were from Sigma Aldrich (Saint Louis, MO).

Methods

Melittin preparation

One milligram of melittin was dissolved in 1mL buffer Hepes 20mM pH 7.4 at 25ºC to maintain the monomeric conformation. The tetrameric melittin conformation was obtained preparing peptide stock solution at 1.8mM in buffer 20mM Hepes pH 7.4 NaCl 250mM. To monitoring the α-helical content of melittin in solution under each experimental conditions, far-UV circular dichroism was recorder.

Nanoparticles preparation

Nanoparticles were prepared by double emulsion solvent evaporation method using power ultrasound. Double emulsion was prepared by two-step emulsification process. In the first step, in order to make the primary emulsion (W1/O), 20 mg poly(lactic-co-glycolic acid) (PLGA, MW 17,000) were dissolved in 1.5mL of ethyl acetate and 20mg of Lutrol F 68 (Poloxamer 188, BASF) properly to form a clear solution. This mixture was homogenized properly using ultrasonic homogenizer for 90 s (Branson Ultrasonics Corp, Danbury, CT, USA). In the second step, the primary emulsion (W1/O) was dispersed in the outer aqueous phase (W2) containing magnesium chloride 3.0 % w/w. This mixture was homogenized via ultrasonic homogenizers for 90s which

produced double emulsion (W1/O/W2). Afterword, the organic solvent evaporation from dispersed droplets via rotary evaporator (Heidolph instruments GmbH and Co. Alemania) has led to solidified PLGA nanoparticles. Then 40μL of an aqueous solution of tetrameric melittin [1.8mM] was added to the preformed nanoparticles and the residual free (unbound) melittin washed out by centrifugation at 35,000 rpm for 3 h.

Hydrodynamic size measurement

The mean diameter and polydispersity index (PDI) of the nanoparticles were measured by dynamic light scattering (DLS) using a ZS90 (Malvern Instruments, R.U.) working at an angle of 90°. The analysis was performed right after the preparation of the nanoparticle dispersions. Before analysis, the samples were diluted 50 times in Milli-Q water to reach a level of light scattering signal recommended by the supplier of the light scattering apparatus. Each sample was analyzed in triplicate.

Determination of melittin assembled in nanoparticles

Samples of NPs loaded with melittin were analyzed by measuring the fluorescence intensity emitted by tryptophan 19 (excitation, 280nm; emission, 351nm) and interpolating the value on a calibration curve prepared for this purpose ($y = 49.036x + 1.17$; $R^2 = 0.9882$). The calibration curve was obtained measuring the emission of melittin in buffer Hepes 20mM pH 7.4. The amount of melittin incorporated in NP was also confirmed by Bradford assay for which, the melittin-nanoparticles

suspension were centrifuge at 10,000rpm for 30min to remove the unbound melittin. The melittin in the supernatant was quantified as recommended by the manufacturer (Bio-Rad Protein Assay).

Circular dichroism

Conformational changes occurring once the peptide was assembled into nanoparticles were monitored by circular dichroism (CD) spectroscopy. CD spectra were registered in a J-1100 spectropolarimeter (JASCO, Easton, MD) equipped with a Koolance Peltier-type holder for temperature control at 25ºC. All spectra were recorded in 0.2nm wavelength increments with a 4s response and a bandwidth of 1nm. The secondary structure of the assembled and native melittin was assessed from spectra registered over the 190-240nm (far-UV) at a scan rate of 50nm/min. Each spectrum is the average of 5 scans with a full scale sensitivity of 50mdeg. All spectra were corrected for background by subtraction of appropriate blanks and were smoothed making sure that the overall shape of the spectrum remains unaltered. Measurements were made in a 0.1cm cuvette with melittin solutions (70μM) or a diluted suspension of nanoparticles containing 100μg of peptide per milliliter. The samples were equilibrated in buffer Hepes 5mM pH 7.4. Helix content of peptide was assumed to be directly proportional to mean residue ellipticity (MRE) at 222nm $[\theta]_{222}$. One hundred percent helicity was calculated using the formula $^{max}[\theta]_{222} = -40{,}000 \times [(1 - 2.5/\eta)] + (100 \times T)$, where η is number of amino acid residues and T is temperature in ºC (15,16). Percentage helicity was then calculated as $100 \times [\theta]_{222} / {}^{max}[\theta]_{222}$.

153 *Intrinsic fluorescence*

154 The polarity of the microenvironment around tryptophan residue at position 19th was investigated by
155 measuring the intrinsic fluorescence of melittin in buffer and melittin-PLGA-NP after sample
156 excitation with 280nm UV radiation. Emission spectra were registered from 300 to 500nm in a
157 LS45 spectrofluorometer (Perkin-Elmer Inc.) with 1cm cells. Nanoparticle and melittin samples
158 were prepared in buffer Hepes 50mM pH 7.4 NaCl 150mM and the protein concentration was
159 adjusted to 15 μg/mL.

160

161 *Vesicle preparation*

162 We used the mixture PC/PE/PS (50:40:10 w/w) to simulate membranes healthy mammary epithelial
163 cells and the mixture PC/PE/PS/PA (50:25:15:10 w/w) to resemble the membranes of breast cancer
164 cells. As representative compounds of erythrocyte membrane we used PC liposomes. The lipids
165 were mixed in chloroform/methanol 2:1 (v/v) and the mixture was dried under a N_2 stream and then
166 for 2 h in a vacuum chamber to form a thin film which was later resuspended by addition of 1mL of
167 50mM Hepes buffer pH 7.4, containing 150mM NaCl and incubated for 2h with eventual vortexing
168 at 25ºC for each lipid mixture. Large unilamellar vesicles (LUVs) were prepared using a Mini-
169 extruder (Avanti Polar Lipids) with 10mm diameter drain discs and 0.1 □m diameter Nu
170 Track-Etched membranes (Whatman) passing the multilamellar membrane vesicles suspension 11
171 times through the filters at 25ºC.

172

173

Leakage of vesicle aqueous contents

Melittin-induce release of aqueous vesicle content was measured by using the ANTS/DPX assay. PC, PC/PE/PS (50:40:10 w/w) or PC/PE/PS/PA (50:25:15:10 w/w) vesicles were prepared by extrusion of lipid suspension prepared in 50mM Hepes buffer, pH 7, containing 30mM NaCl, 12.5mM of ANTS and 45mM DPX as a quencher. Vesicles were separated from unencapsulated material on a Sephadex G-75 column (Sigma-Aldrich) by using 50mM Hepes pH 7, containing 150mM NaCl, as elution buffer. The final lipid concentration after exclusion chromatography was determined by phosphorus assay (17). In a typical leakage assay, a given volume of melittin or melittin-PLGA-NP was added from a concentrated solution to the ANTS/DPX-loaded vesicles at 75μM lipid. The resulting leakage was then followed by measuring the increase in fluorescence emission intensity at 536nm, upon excitation at 353nm, in a LS45 Perkin-Elmer spectrofluorometer. Complete (100%) release was achieved by the addition of 0.5% Triton X-100. All experiments were conducted at 25ºC, and the apparent percentage of leakage was calculated according to the following Equation:

$$\text{Leakage (\%)} = 100 \times (F - Fo) / (Ft - Fo)$$

where F and Ft represent the fluorescence intensity before and after the addition of detergent, respectively, and Fo represents the fluorescence of intact vesicles.

Results and Discussion

PLGA-Nanoparticles characterization

Melittin was encapsulated in poly(lactic-co-glycolic acid)-nanoparticles (PLGA-NP) by the water-in-oil-in-water ($W_1/O/W_2$) emulsion method optimized in our laboratory as previously described (18). We characterized our PLGA-NP by undertaking the analysis of nanoparticle size and evaluating the amount of melittin adsorb in the PLGA-NP surface. DLS data indicated that NP size was 85 ± 20 nm (n=3) with a narrow size distribution (Figure 1A) while the PDI < 0.1 confirmed that the particle was a typical monodisperse system. It is interesting to note that the incorporation of melittin in the PLGA nanoparticles leads to a narrow size distribution (Figure 1B) and to an increase of NP size of 110 ± 20 nm (n=3) as a result of adsorption of melittin at the nanoparticle surface.

Melittin basic amino acids (I^{20}-K^{21}-R^{22}-K^{23}-R^{24}-Q^{25}) are responsible for an electric interaction with the lutrol polar group present in NP, leading to a small increase in average particle size. Similar results had been observed by other authors using three kinds of polymers (19). It is well established that free melittin monomer is essentially a random coil molecule, whereas it displays a high α-helix content when it is bound to membranes (20). To evaluated the secondary structure of melittin in the PLGA-NP CD spectroscopy was performed, once establish the amount of melittin incorporated into nanoparticle surface.

Determination of melittin in PLGA-Nanoparticles

To characterize the properties of the peptide incorporated into nanoparticles it is necessary to precisely determine the protein content in nanoparticle suspension. Therefore, samples of NPs (prepared as described in the Experimental section) were analyzed by two different methods: Bradford assay and direct determination of melittin incorporated in nanoparticles by analyzing the fluorescence intensity emitted by tryptophan 19 (excitation, 280nm; emission, 351nm) and interpolating the value on a calibration curve prepared for this purpose ($y = 49.036x + 1.17$; $R^2 = 0.9882$). As determined by the Bradford assay, the protein content in NP was 175μg ± 2μg and as determined by fluorescence intensity method, the amount of melittin incorporated was 170μg ± 0.5μg of the final nanoparticle suspension (average of three individual batches of NPs). The percentage yield of melittin PLGA-NP was found to be 85%. Similar yields have been reported by Cui *et al.* (2005) for the preparation of PLGA nanoparticles by the double emulsion method. The mass ratio for vehicle: active was calculated and found that for every 40 mg of total solids (polymer and surfactant) is feasible to incorporate 170 μg of peptide. These values are consistent with those reported by other authors, which had evaluated the ability of interaction between PLGA particles and peptides or proteins and have shown a high interaction (21). However, it should be noted that the emission spectrum of melittin loaded PLGA-NP (Figure 2) appears to be blue-shifted (change in emission from 351nm to 331nm) and more intense when compared with the spectrum of melittin in solution; these differences in fluorescence properties are indicative of changes in the environment of aromatic residues that occur during the adsorption process. Specifically, the aforementioned spectral blue shift suggests that Tryptophan (Trp) residue at position 19 is less exposed to the

aqueous solvent in NP than native melittin. Similar results were observed for α-lactoalbumin when assembled into NPs (22). In the melittin tetramer, the intrinsic solvation probe of Trp is located at the junction between 2 α-helical monomers and is partially buried. However, Trp is fully exposed to the solvent environment in the helical monomer. Raghuraman *et al*., reported that melittin tetramer is stabilized by increasing concentration of NaCl. The effect of NaCl on increasing the amount of tetramer starts around 0.25 M and the effect appears mainly for pH values less than 8 (23) so, at the conditions used in this work, the tetrameric structure was form before addition to nanoparticles, and remains stable after the addition to NP. To confirm this, it was monitored the α-helical content in PLGA-NP loaded with melittin by circular dichroism at 222nm.

Conformational changes in melittin upon adsorption to nanoparticles

The far-UV (205 – 250 nm) CD spectrum of monomeric and tetrameric melittin are shown in Figure 3. Monomeric melittin shows a minimum at 205nm, indicating the absence of any significant secondary structure in the peptide. The far UV spectrum of tetrameric melittin displays a strength α-helical configuration with a broad negative band centered on 222nm. It is well establish that increasing concentration of peptide and NaCl stabilizes melittin tetramer, so the stock solution prepared in this work agrees with these two conditions allowing melittin self-aggregation. Similar spectra were obtained by other authors in buffer Tris 20mM pH 7.4 150mM NaCl at 25ºC and peptide concentration of 0.5mM (24, 25). By increasing peptide and NaCl concentration the conformation of melittin changes from a mainly random-coiled structure, with only 21% of α-helix,

to a mainly helical one with 56%. Our observation is in line with the experimentally measured helicity obtained by other authors (26).

We compared the CD spectra of tetrameric melittin once incorporated in PLGA-NP to determine whether similar changes in the secondary structure of melittin occurred upon binding to the nanoparticles. Because control of PLGA-NP sample gave a flat ellipticity trace (see open circles in Figure 4), the CD band observed in melittin PLGA-NP can be attributed to the peptide present therein. The overall characteristics (i.e., peak position and ellipticity magnitude) of the spectrum clearly reflects the large number of α-helix regions found in this macromolecule, with double negative peaks at 222nm and 208nm and an helical content of 40%. Interestingly, the secondary structure of melittin PLGA-NP is similar to that reported as the CD spectra of tetrameric melittin at 0.5mM peptide concentration, suggesting that tetramer formation remains stable after incorporation of peptide to NP. These results confirm that melittin interacts with the PLGA-NP and exists as a stably integrated component of the NP in its tetrameric form even in the absence of a monolayer membrane surrounding the nanoparticle. Using a hybrid melittin cytolytic peptide (27) and a different nanoparticle composition (28) other authors obtained similar results. We then assessed the functional activity of melittin bound to nanoparticles by determining pore formation upon interaction with liposomes that resembles breast cancer cell.

Kinetics of liposome leakage

Vesicles with different structures are used extensively in drug delivery and combinatory chemotherapeutic systems and can also be used to study artificial cell formation, which primitively

mimics the membrane-based structure of eukaryotic cells (29). Alterations of phospholipid profiles have been associated to disease and specific lipids may be involved in the onset and evolution of cancer. Doria *et al*., reported a lipidomic analysis of phospholipids from human mammary epithelial cells and breast cancer cell lines (MCF10A, T47-D and MDA-MB-231) using off-line thin layer chromatography (TLC) validated by hydrophilic interaction liquid chromatography-MS. Differences in phosphatidylethanolamine (PE) and phosphatidylserine (PS) content relative to total amount of phospholipids was highest in non-malignant cells while phosphatidic acid (PA) was present with highest relative abundant in metastatic cells (30). The phospholipids mixture used in this work for preparing liposomes where PC/PE/PS (50:40:10 w/w) to mimic membranes healthy mammary epithelial cells and the mixture PC/PE/PS/PA (50:25:15:10 w/w) to resemble the membranes of breast cancer cells. As representative compound of erythrocyte membrane, we used vesicles containing 100% PC. Membrane disruption by melittin PLGA-NP was characterized using a dye efflux assay. The assay is based on measuring the increase fluorescence that results from leakage of a quenched dye that is loaded into liposomes. The quenching property of fluorescence dye permits leakage from liposomes to be monitored continuously and is sensitive to small perturbation in the bilayer (31). Large unilamellar vesicles (LUVs) were filled with ANTS/DPX at concentration at which ANTS fluorescence is quenched by DPX. Upon leakage from the vesicle, quenching of the dye is relieved and a fluorescence signal is observed. PLGA-NP loaded with melittin induces leakage of the aqueous content from each kind of LUVs tested. The effect of phospholipid composition on the lytic power of melittin-PLGA-NP is shown in Figure 5. Initially, no fluorescence is observed in all cases since the high concentration (45mM) of DPX used resulted

in quenching of ANTS fluorescence. Upon addition of melittin-PLGA-NP, the entrapped ANTS/DPX were released into the buffer due to membrane perturbation, leading to the dilution of the DPX quenching effect, increasing ANTS fluorescence. The extent of increase in fluorescence intensity is a measure of the lytic power of melittin in a given membrane environment. As is evident from the figure the lytic efficiency of NP-melittin in different vesicles is clearly dependent on the composition of the membrane: slightly higher lytic activity is observed in the presence of PA at any peptide concentration an also, the membrane perturbation effect occurs immediately after being added the peptide (Figure 5A). In the case of liposomes that resembles healthy mammary epithelial cells (PC/PE/PS 50:40:10 w/w) it can be observed that with the last three peptide concentrations evaluated, achieve the maximum lytic activity takes a few seconds before fluorescence intensity reaches a plateau indicating that no further release occurs after a certain period (Figure 5B). For liposomes that resemble erythrocyte membrane (PC vesicles), the natural target of melittin, the kinetics also show that achieve the maximum lytic activity takes a few seconds before fluorescence intensity reaches a plateau. Figure 5C shows how from 10μM peptide concentration, takes longer to disrupt the lipid bilayer. In all liposomes used in this work, the time required for melittin-PLGA-NP to produce maximum leakage, as well as the maximal amount o fluorescence liberated were both dependent on peptide concentration.

The lipid disruption properties of melittin-PLGA-NP are summarized in Figure 6, it can be observed how the incorporation of melittin to PLGA-NP do not alter the cytolytic ability of this peptide on any of the phospholipid vesicles analyzed. Melittin-PLGA-NP were able to disrupt 50% of the PC LUVs at concentrations of around 2μM. The NP loaded with tetrameric melittin were more

effective inducing leakage from PC/PE/PS (50:40:10 w/w) and PC/PE/PS/PA (50:25:15:10 w/w) at around 1.2μM and 1.8μM respectively.

It has been reported that under similar experimental conditions, free melittin originate leakage from zwitterionic liposomes at around 0.25μM and at 0.4μM from liposomes containing 10% molar of negatively charged phospholipids (32-34) which represents an increase of about 8% in peptide concentration comparing with our results for zwitterionic liposomes and an increase of 3% for liposomes containing PS and 5% of liposomes with PA; so the tetrameric conformation of melittin incorporated in PLGA nanoparticles form a hydrophobic patch when a helical region is structured, reducing the lytic activity from zwitterionic lipids while retains its cytotoxic activity against anionic membranes. These results are in accordance with observations made by Pandey et al. (2010) who reported increasing cell selectivity using a Leu9Ala mutation which exhibited significantly reduce hemolytic activity than that of native melittin, while the analogues of melittin showed comparable antibacterial activities to melittin against Gram-positive and –negative bacteria (35).

It is important to note that the lytic activity of our tetrameric melittin-PLGA-NP is more cytotoxic than other melittin-NP system reported. Huang *et al.* (2013) designed a hybrid cytolytic peptide, α-melittin in which the N-terminus of melittin is linked to the C-terminus of an amphipathic α-helical peptide via a GSG linker. These α-melittin-NPs induced minimal hemoglobin release at concentration of 50μM while the cytotoxicity in tumor cells was reached at 11.26μM. This represents a tolerance of about 10 times more than our system for PC membranes and around 2 times more for membranes containing anionic phospholipids. Soman *et al.* (2009) observed a more protective action against red blood cell hemolysis with the use of lipid-based melittin-

perfluorocarbon nanoparticles; they report that even a concentration of 25μM nanoparticle-melittin only elicited 10% hemolysis. So it is clear that to reduce melittin hemolytic activity is necessary to shield its hydrophobic N-terminal segment either trough structural changes or alteration in melittin sequence or by conjugation with other hydrophobic molecules. In this light, our results demonstrated that is therefore possible to selectively favor melittin aggregation and preserve the complex peptide structure in an active form once incorporated to PLGA-NP. However we need to improve our formulation system to reduce even more melittin lytic activity on membrane model systems that aims to conduct hemolytic assays using red blood cells.

Conclusion

To summarize, our goal in this study was to formulate stable high payload PLGA particles as nanovehicles for tetrameric melittin and evaluate its utility as a cancer chemotherapeutic agent in a model bilayer membrane system. Our results indicate that melittin tetrameric conformation in PLGA-NP is able to slightly reduce the lytic activity of this peptide over mammalian cell membrane mimetic model membranes supporting a crucial role for hydrophobic region to permeabilize zwitterionic liposomes. However the reduction observed it is not enough for *in vivo* administration. It is to be mentioned that our nanoparticle-system induced significant and very similar leakage in the PC/PE/PS and PC/PE/PS/PA lipid vesicles, which indicate that tetrameric melittin conformation retain the ability to permeabilize the negatively charged lipid membranes. Additional research is needed to investigate the mechanisms by which tetrameric melittin-PLGA-NP interact and perturb lipid bilayers. We need to improve our NP formulation to reduce even more melittin lytic activity

that aims to conduct hemolytic assays using red blood cells and also cell viability assays against endothelial and breast cancer cell lines to translate our findings into useful therapeutic potential.

Acknowledgments

This research was financially supported by the Consejo Nacional de Ciencia y Tecnología (CONACYT) Proyect No. C.B. 2014 236834.

Conflicts of Interest

None declared.

Author Contributions

Conceived and designed the experiments: A.G.H., A.Ch.M.; performed nanoparticle preparation and leakage experiments: A.M.A.; performed CD experiments: A.G.H.; analyzed the data and wrote the paper: A.G.H. All authors read and approved the final manuscript.

References

1. Habermann, E. (1977). Bee and wasp venoms. Science. 177, 314-322. PMID: 4113805.
2. Raghuraman, H.; Chattopadhyay, A. (2004). Effect of micellar charge on the conformation and dynamic of melittin. *Eur Biophys J* 33, 611-622. DOI: 10.1007/s00249-004-0402-7.

3. Raghuraman, H.; Chattopadhyay, A. (2004). Influence of lipid chain unsaturation on membrane-bound melittin: a fluorescence approach. *Biochem et Biophys Acta* 1665, 29-39. DOI: 10.1016/j.bbamem.2004.06.008

4. Raghuraman, H.; Chattopadhyay, A. (2007). Melittin: a membrane-active peptide with diverse functions. *Biosci Rep* 27, 189-223. DOI: 10.1007/s10540-006-9030-z

5. Pott, T.; Maillet J.C.; Abad, C.; Campos, A.; Dufourcq, J.; Dufourc, E.J. (2001). The lipid charge density at the bilayer surface modulates the effects of melittin on membranes. *Chem and Phys of Lipids* 109, 209-223. PMID: 11269939

6. Allende, D.; Simon, S.A.; McIntosh T.J. (2005). Melittin-Induced bilayer leakage depends on lipid material properties: evidence for toroidal pores. *Biophys J*. 88, 1828-1837. DOI: 10.1529/biophysj.104.049817

7. Yang, D.; Harroun, T.A.; Weiss T.M.; Ding L.; Huang H.W. (2001). Barrel-stave model or toroidal model? A case study on melittin pores. *Biophys J.* 81, 1475-1485. DOI: 10.1016/S0006-3495(01)75802-X

8. Shigeri, Y.; Horie, M.; Yoshida, T.; Hagihara, Y.; Imura, T.; Inagaki, H.; Haramoto, Y.; Ito, Y.; Asashima, M. (2016). Physicochemical and biological characterizations of Pxt peptides from amphibian (Xenopus tropicalis) skin. *J. Biochem.* 159(6): 619-629. DOI: 10.1093/jb/mvw003.

9. Gajski, G.; Cimbora-Zovko, T.; Osmak, M.; Garaj-Vrhovac, V. (2011). Bee venom and melittin are cytotoxic against different types of tumor and non-tumor cell lines in vitro. *Cancer Res. J.* 4, 159-174. NLM ID: 101560428

10. Liu, S.; Yu, M.; He, Y.; Xiao, L.; Wang, F.; Song, C.; Ling, C.; Xu, Z. (2008). Melittin prevents liver cancer cell metastasis through inhibition of the Rac1-dependent pathway. *Hepathology* 47, 1964-1973. DOI: 10.1002/hep.22240

11. Jeong, YJ.; Choi, Y.; Shin JM.; Cho, HK.; Kang, JH.; Park, KK.; Choe, JY.; Chang, YC. (2014). Melittin suppresses EFG-induced cell motility and invasion by inhibiting PI3K/Akt/mTOR signaling pathway in breast cancer cells. *Food and Chemical Toxicity* 68, 218-225. DOI: 10.1016/j.fct.2014.03.002

12. Pan, H.; Soman, N.R.; Sclesringer, P.H.; Lanza, G.M.; Wickline, S.A. (2011). Cytolytic peptide nanoparticles (NanoBees) for cancer therapy. *Wiley Interdiscp. Rev. Nanomed. Nanobiotechnol* 3, 318-327. DOI: 10.1002/wnan.126

13. Bala, I.; Hariharan, S.; Kumar, M.N. (2004). PLGA nanoparticles in drug delivery: The sate of the art. *Crit. Rev Ther Drug Carrier Syst*. 21, 387-422. PMID: 15719481

14. Park, M.; Kim, J.; Jeon, J.; Park, J.; Lee, BJ.; Suh, G.H. and Cho, Ch.W. (2015). Preformulation studies of bee venom for the preparation of bee venom-loaded PLGA particles. Molecules, 20, 15072-15083. DOI:10.3390/molecules200815072

15. Scholtz, J.; Qian, H.; York EJ.; Stewart, JM.; Baldwin, R.L. (1991). Parameters of helix-coil transition theory for alanine-based peptides of varying chain lengths in water. Biopolymers 31(13), 1463-1470.

16. Jamasbi, E.; Batinovic, S.; Sharples, R.; Sani, MA; Robins-Bowne, RM; Wade, JD; Sparovic, F.; Hossain, MA. (2014). Melittin peptides exhibit different activity on different cells and model membranes. Amino Acids 46, 2759-2766.

17. Rouser, G.; Siakotos, A.N.; Fleischer, A.S. (1996). Quantitative analysis of phospholipids by thin-layer chromatography and phosphorus analysis of spots. *Lipids* 1, 85-86. DOI: 10.1007/BF02668129

18. Gonzalez, E.; Gonzalez, A.; Castro, R.; Luna, H.; Chavez, A. (2015). Implementacion de la tecnica de doble emulsion para la microencapsulacion polimerica de moleculas ionicas. *Rev. Ib. Ci.,* 2(4), 117-125. ISSN: 2334-2501

19. Cui, F.; Cun, D.; Tao, A.; Yang, M.; Shi, K.; Zhao, M.; Guan, Y. (2005). Preparation and characterization of melittin-loaded poly (DL-lactic acid) or poly (DL-lactic-co-glycolic acid) microspheres made by the double emulsion method. *J. Con. Rel*. 107, 310-319. PMID: 16255081

20. Vogel, H.; Jähnig F. (1986). The structure of melittin in membranes. *Biophys J*. 573-582. DOI: 10.1016/S0006-3495(86)83497-X

21. Arroyo-Maya, I.J.; Hernandez-Sanchez, H.; Jimenez-Cruz, E.; Camarillo-Cadena M.; Hernandez-Arana, A. (2014) α-Lactoalbumin nanoparticles prepared by desolvation and cross-linking: Structure and stability of the assembled protein. *Biophys Chem*. 193-194, 27-34. DOI: 10.1016/j.bpc.2014.07.003

22. Raghuraman, H.; Ganguly, S.; Chattopadhyay A. (2006). Effect of ionic strength on the organization and dynamics and membrane-bound melittin. *Biophys Chem*. 124 (2), 115-124. DOI: 101016/j.bpc.2006.06.011

23. Wilcox, W.; Eisenberg, D. (1992). Thermodynamics of melittin tetramerization determined by circular dichroism and implications for protein folding. *Protein Science*, 1, 641-653. DOI: 10.1002/pro.5560010510.

24. Goto, Y.; Hagihara, Y. (1992). Mechanism of the conformational transition of melittin. *Biochemistry*, 31, 632-738.

25. Liao, C.; Myvizhi, E.; Zhao, J.; Slimovitch, J.; Schneebeli, S.; Shelley, M.; Shelley, J.; Li, J. (2015). Melittin aggregation in aqueous solutions: insight form molecular dynamics simulation. *J Phys Chem B.*, 119 (33), 10390-10398.

26. Takahashi, T.; Nomura, F.; Yokoyama, Y.; Tanaka-Takaguchi, Y.; Homma, M.; Takaguchi K. (2013). Multiple membrane interactions and versatile vesicle deformations elicited by melittin. *Toxins*, 5, 637-664. DOI: 10.3390/toxins5040637

27. Huang C.; Jin, H.; Qian, Y; Qi, S.; Luo, H.; Luo, Q.; Zhang, Z. (2013). Hybrid melittin cytolytic peptide-driven ultrasmall lipid nanoparticles block melanoma growth in vivo. *ACS Nano* 7 (7), 5791-5800. DOI: 10.1021/nn400683s

28. Soman, N.R.; Lanza, G.M.; Heuser, J.M.; Schlesinger, P.H.; Wickline S.A. (2008). Synthesis and characterization of stable fluorocarbon nanostructures as drug delivery vehicles for cytolytic peptides. *Nano Letters* 8 (4), 1131-1136. DOI: 10.1021/nl073290r

29. Paleos, C.M.; Tsiorvas, D.; Sideratou, Z. (2012). Preparation of multicompartment lipid-based systems based on vesicle interactions. *Langmuir* 28, 2337-2346. DOI: 10.1021/la2027187

30. Doria, M.L.; Cotrim, C.Z.; Simoes, C.; Macedo, P.D.; Dominguez R. and Helguero, L.A. (2013). Lipidomic analysis of phospholipids from human mammary epithelial and breast cancer cell line. *J. Cell Physiol* 228, 457-468. DOI: 10.1002/jcp.24152

31. Ralston, E.; Hjelmeland, H.M.; Klausner, R.D.; Winstein, J.N.; Blumenthal, R. (1981). Carboxyfluorescein as a probe for liposome-cell interactions. Effect of impurities, and purification of the dye. *Biochem et Biophys Acta* 649, 133-137. DOI: 10.1016/0005-2736(81)90019-5

32. Soman, R.N.; Baldwin, S.L.; Hu, G.; Marsh, J.N.; Lanza, G.M.; Heuser, J.E.; Arbeit, J.M.; Wickline, S.A.; Schlesinger, P.H. (2009). Molecularly targeted nanocarriers deliver the cytolytic peptide melittin specifically to tumor cells in mice, reducing tumor growth. *J. Clin. Invest.* 119, 2830-2842. DOI: 10.1172/JC138842

33. Van den Bogaart, G.; Velasquez Guzman, J.; Mika, J.T.; Poolman, B. (2008). On the mechanism of pore formation by melittin. *J. Biol. Chem.* 49, 33854-33857. DOI: 10.1074/jbc.M805171200

34. Higashino, Y.; Matsui, A.; Ohki, K. (2001). Membrane fusion between liposomes composed of acidic phospholipids and neutral phospholipids induced by melittin: A differential scanning calorimetric study. *J. Biochem.* 130 (3): 393-397. PMID: 11530015.

35. Pandey, B.K.; Ahmad, A.; Asthana, N.; Azmi, S.; Srivastava, R.M.; Srivastava, S.; Verma, R.; Vishwakarma, A.L.; Ghosh, J.K. (2010). Cell-Selective lysis by novel analogues of melittin against human red blood cells and Escherichia coli. *Biochemistry* 49, 7920-7929. DOI: 10.1021/bi100729m

Legends of figures

Figure 1. Mean size distribution of PLGA-nanoparticles (A) and melittin PLGA-NP (B). The analysis was performed right after the preparation of the nanoparticle dispersions. The samples were diluted 50 times in Milli-Q water to reach a level of light scattering signal recommended by the supplier of the light scattering apparatus.

Figure 2. Fluorescence emission spectra of PLGA-nanoparticles loaded with melittin. Intrinsic tryptophan fluorescence of melittin in solution (○), fluorescence of melittin-PLGA-NP (●) and polymeric nanoparticles (●) are shown. The excitation wavelength was 280nm and the final peptide concentration was 20μg/mL.

Figure 3. Circular dichroism spectra of monomeric (●) and tetrameric melittin (○). The peptide concentration used for the CD analysis was [70μM]. Data are reported as mean residue ellipticity. Monomeric and tetrameric melittin was prepared as described in methods.

Figure 4. Circular dichroism spectra of free PLGA-Nanoparticles (○) and diluted suspension of tetrameric melittin-PLGA-Nanoparticle containing 100μg of protein per milliliter (●). The samples were equilibrated in buffer Hepes 5mM pH 7.4. Data are reported as mean residue ellipticity.

Figure 5. ANTS/DPX release induced by PLGA-NP loaded with melittin from PC/PE/PS/PA (50:25:15:10 w/w) vesicles (A); PC/PE/PS (50:40:10 w/w) liposomes (B) and PC vesicles (C). Peptide concentration assayed were (from dark circles to diamonds) 1.5, 2.5, 3, 5, 7, 10 and 14μM and is indicated in the figure as the first arrow. The final lipid concentration was 75μM. Peptide-induced liberation of the fluorophores ANTS from the vesicles was followed by monitoring fluorescence emission using excitation and emission wavelengths of 353 and 536nm, respectively. The percentage of leakage induced by any given peptide concentration was estimated taking as a reference the maximum possible leakage, obtained after addition to the samples of an aliquot of Triton X-100 (final concentration of 0.5%, v/v) indicated as the second arrow in each figure.

Figure 6. Effect of melittin-PLGA-NP on the leakage from PC (○) PC/PE/PS (50:40:10 p/p) (●) and PC/PE/PS/PA (50:25:15:10 w/w) (●) LUVs. Peptide concentration assay were 0.6, 0.8, 1.2, 1.8, 2.4, 3.6, 4.8μM and the final lipid concentration was 25μM. Peptide-induced liberation of the fluorophore ANTS from the vesicles was followed by monitoring fluorescence emission using excitation and emission wavelengths of 353nm and 536nm respectively. The percentage of leakage induced by any given peptide concentration was estimated taking as a reference the maximum possible leakage obtained after addition to the samples of an aliquot of Triton X-100 (final concentration 0.5% v/v). The typical error from at least two independent experiment is indicated.

A

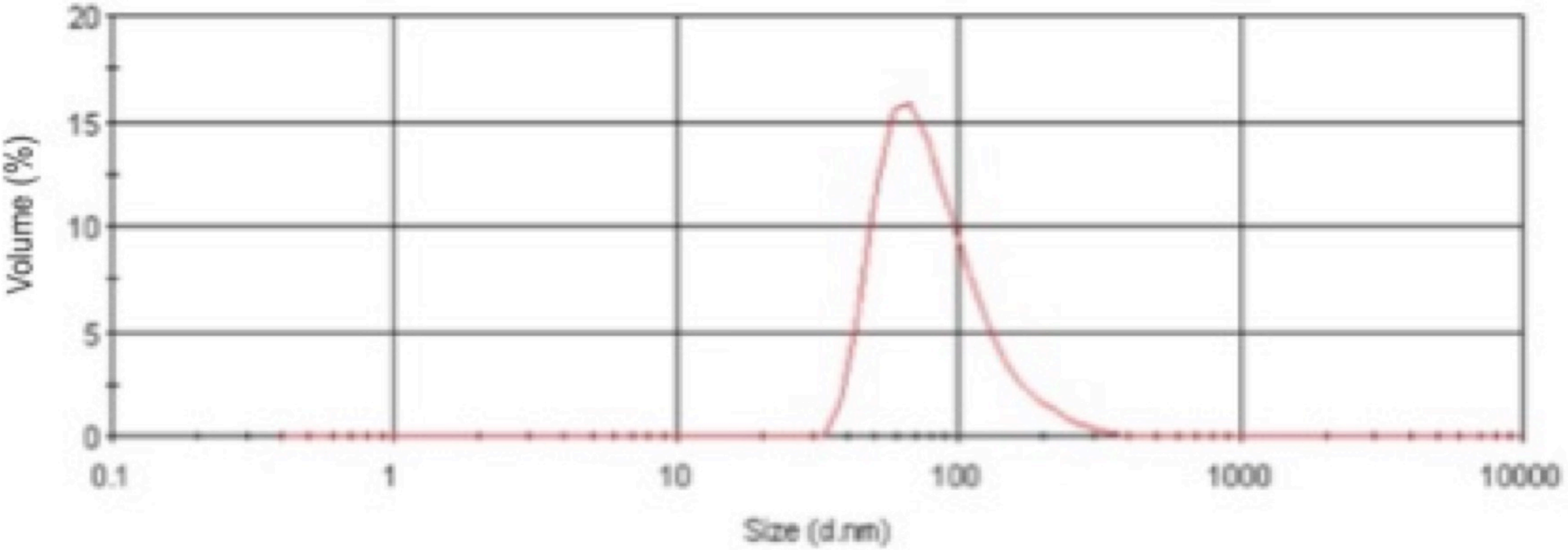
20
15
10
5
0
Volume (%)
0.1
1
10
100
1000
10000
Size (d.nm)

B

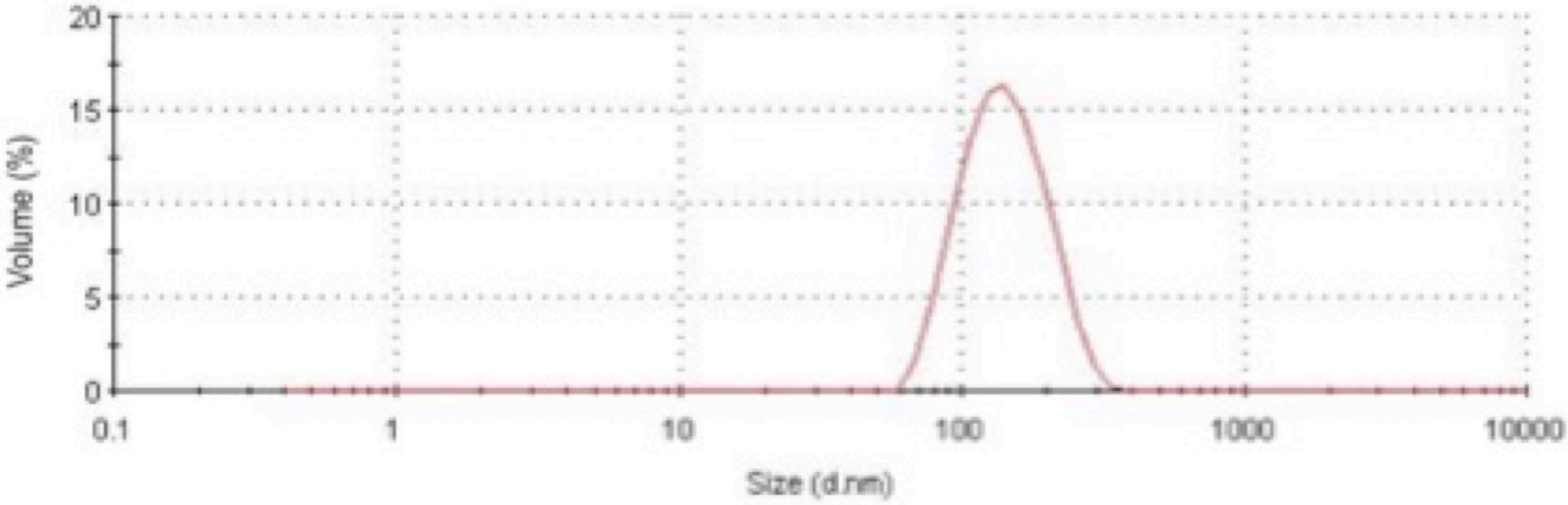
20
15
10
5
0
Volume (%)
0.1
1
10
100
1000
10000
Size (d.nm)

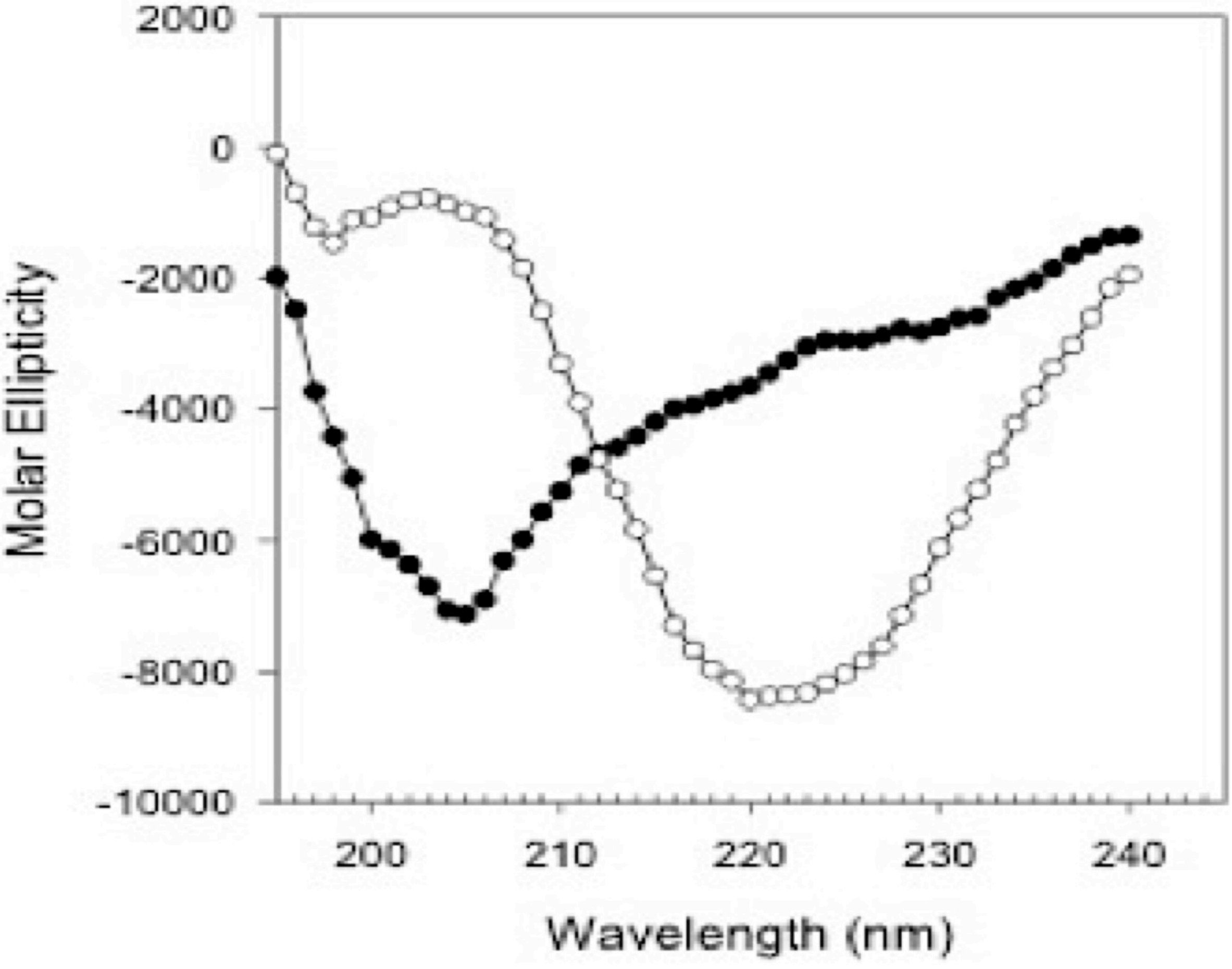
2000
0
-2000
-4000
-6000
-8000
-10000
Molar Ellipticity
200
210
220
230
240
Wavelength (nm)

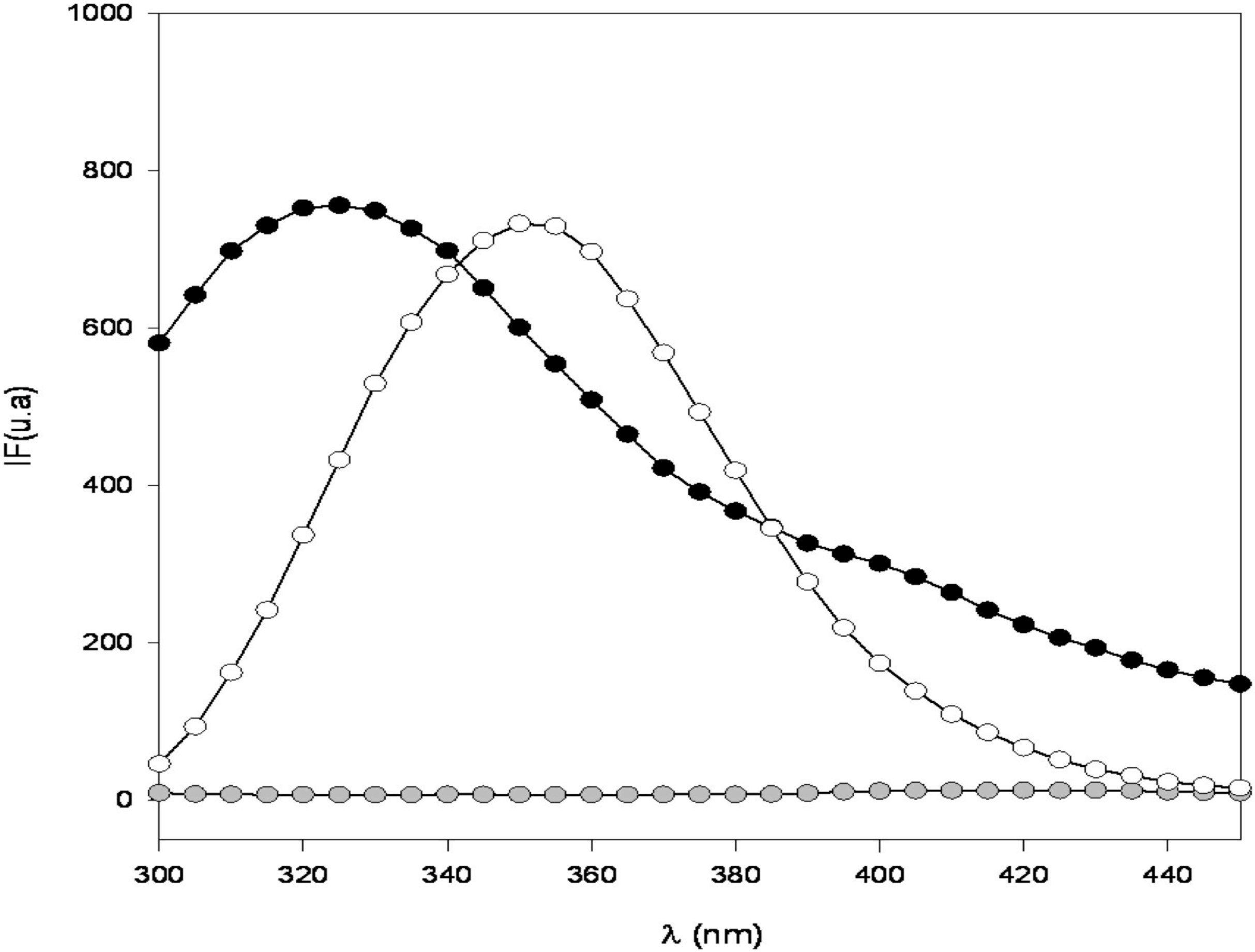
1000
800
600
400
200
0
IF(u.a)
300
320
340
360
380
400
420
440
λ (nm)

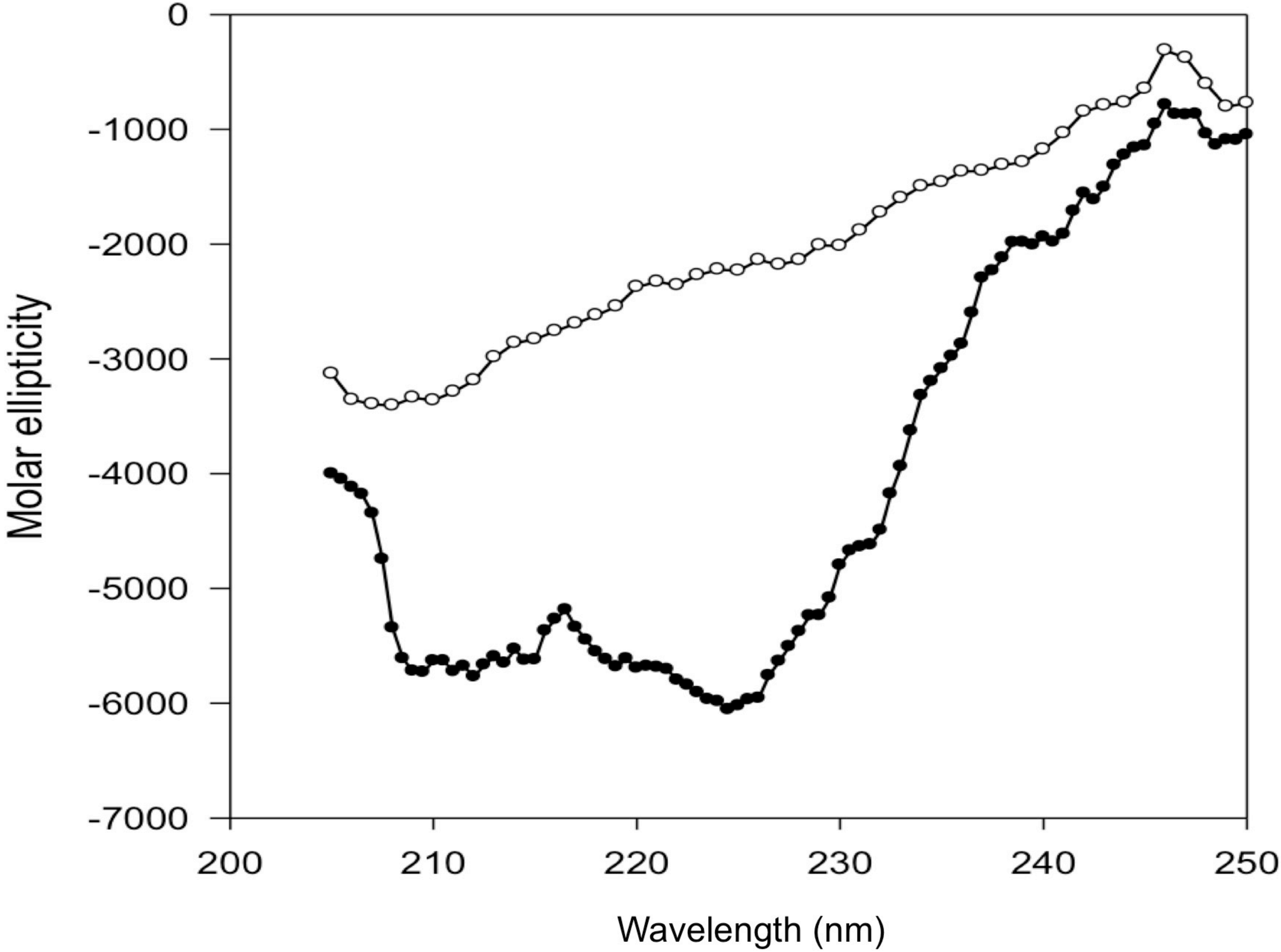
0
-1000
-2000
-3000
-4000
-5000
-6000
-7000
Molar ellipticity
200
210
220
230
240
250
Wavelength (nm)

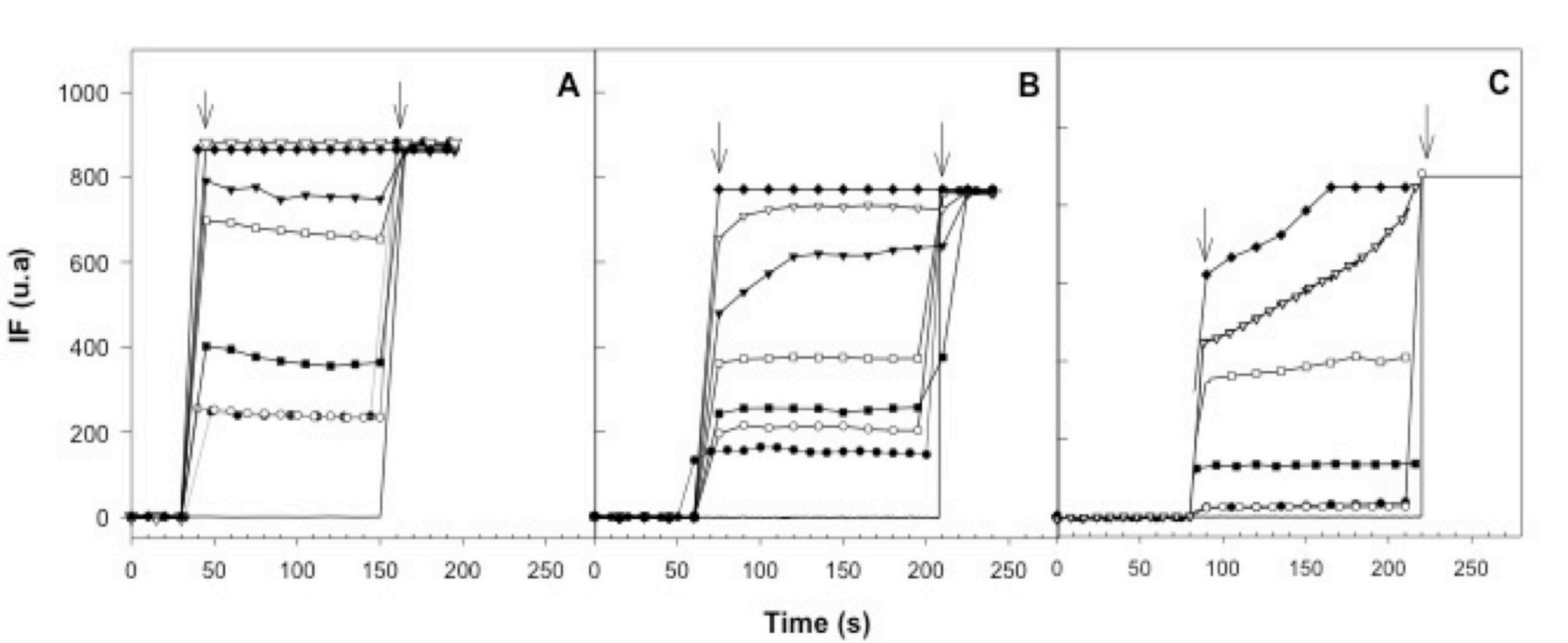
A
B
C
IF (u.a)
Time (s)
0
200
400
600
800
1000
0
50
100
150
200
250

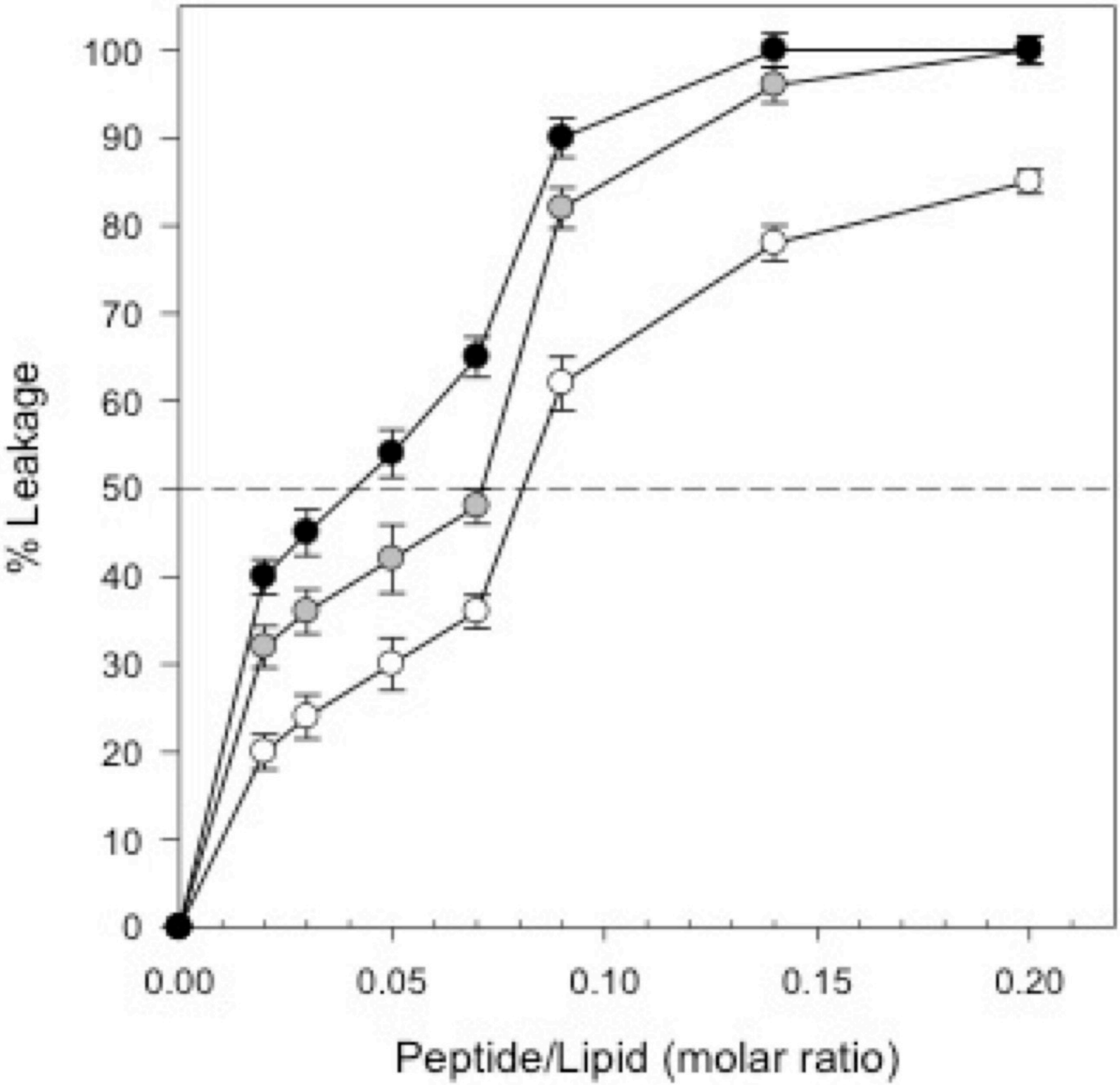
% Leakage
100
90
80
70
60
50
40
30
20
10
0
0.00
0.05
0.10
0.15
0.20
Peptide/Lipid (molar ratio)